

## JP1.2 PROGRESS REPORT ON THE INTEGRATED TERMINAL WEATHER SYSTEM'S GF MOSAIC ALGORITHM

Justin D. Shaw\* and Seth Troxel  
MIT Lincoln Laboratory, Lexington, Massachusetts

### 1. INTRODUCTION<sup>†</sup>

The GF Mosaic algorithm combines information from more than one Doppler radar to provide an improved gust front detection capability at large TRACONs covered by multiple Terminal Doppler Weather Radars (TDWR). Algorithm development and testing is presently taking place at the Dallas/Ft. Worth International Airport (DFW), where the ability to detect gust fronts in the vicinity of the airport is made more difficult because of the location of the DFW TDWR. Radar velocity signatures indicative of gust fronts often degrade or vanish due to Doppler blindness when a gust front becomes radially aligned with the radar. This problem is common at DFW since the DFW TDWR is located northeast of the airport and the most common orientation of cold fronts and thunderstorm outflow boundaries is northeast-to-southwest (Figure 1). The GF Mosaic algorithm is expected to alleviate the gust front detection problem caused by radial alignment at DFW as well as provide a more robust detection capability at all of the Integrated Terminal Weather System (ITWS) sites serviced by more than one TDWR.

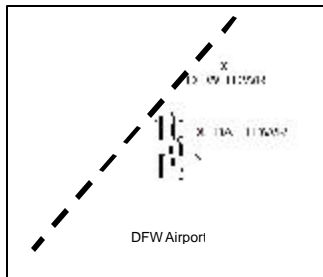


Figure 1. Locations of the DFW TDWR and DAL TDWR with respect to the DFW airport. The dashed line shows the typical orientation of gust fronts.

### 2. GUST FRONT DETECTION STRATEGY

The GF Mosaic algorithm constructs gust fronts from interest images generated by the Machine Intelligent Gust Front Algorithm (MIGFA) (Delanoy,

1993; Troxel, 1994). In MIGFA, pixel maps of evidence called interest images are produced by a set of feature detectors that look for characteristics of gust fronts in the TDWR velocity and reflectivity data. MIGFA fuses the individual interest images from each feature detector to produce a combined interest image. In the typical single-radar configuration, MIGFA proceeds by extracting the gust fronts from regions of high combined interest and reporting those chains that pass a series of tests. In a multi-radar configuration, the GF Mosaic algorithm receives the combined interest image from each MIGFA algorithm and generates a mosaic interest image by fusing the individual combined interest images onto a TRACON domain grid. The size of the TRACON domain is set large enough to encompass the combined coverage of all of the MIGFA algorithms, and the center point is at a location that minimizes the overall domain size. The GF Mosaic algorithm then uses the mosaic interest field to extract gust front chains from the regions of high interest utilizing the standard MIGFA chain extraction and analysis routines.

Several steps are taken to compensate for the asynchronous input of MIGFA interest images into the algorithm. The GF Mosaic processing cycle is driven by arrival of data from a "trigger" radar. The choice of trigger radar is dynamically determined in real-time by comparing the time difference between TDWR scans of the different radars, and choosing the radar whose selection as the trigger results in the smallest time difference for the mosaic. Even with optimum triggering, the time difference between interest images may be large enough that a fast moving gust front may appear as a double line of interest in the mosaic. To avoid generating double gust front detections from misaligned interest, custom smoothing filters are applied to merge double bands of interest into a single band (Figure 2). Subsequent interest "thinning" operations will follow ridges of high interest.

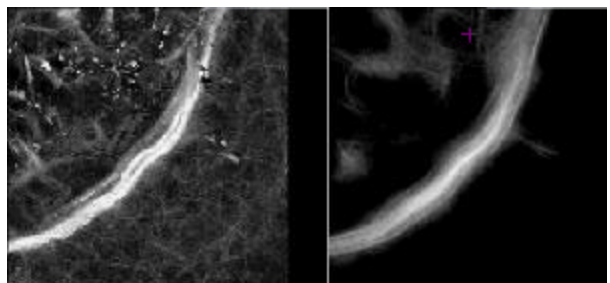


Figure 2. Mosaic interest images showing misaligned interest fields before (left) and after smoothing to merge double interest bands (right).

\*Corresponding author address: Justin Shaw, MIT Lincoln Laboratory, 244 Wood Street, Lexington, MA 02420-9108; e-mail: jdshaw@ll.mit.edu

<sup>†</sup>This work was sponsored by the National Aeronautics and Space Administration under Air Force Contract No. F19628-00-C-0002. The views expressed are those of the authors and do not reflect the official policy or position of the U.S. Government. Opinions, interpretations, conclusions, and recommendations are those of the authors and are not necessarily endorsed by the US Government.

A very useful product of MIGFA is the post-frontal wind estimate, which represents the wind speed and direction that are expected at the airport ten minutes after gust front passage. MIGFA analyzes data from a single TDWR to produce this wind estimate. The GFMosiac algorithm needs to provide the same post-frontal wind information as MIGFA. However, the estimation becomes much more difficult when more than one TDWR is used. Since the detections are made with respect to a grid geometry whose center may or may not be coincident with a radar location, the radial velocity provided by a single TDWR is not clearly interpretable. Furthermore, combining velocity data from multiple Doppler radars is complex and redundant with the 3-dimensional wind field computation already performed by the ITWS Terminal Winds (TWINDS) algorithm. For these reasons, the GFMosiac algorithm intends to utilize ITWS TWINDS data to provide an estimation of the winds behind detected gust fronts.

### 3. USE OF ITWS TERMINAL WINDS (TWINDS)

TWINDS has recently undergone several important enhancements in an effort to provide an improved wind field product. While the complete extent of the algorithm modifications is beyond the scope of this paper, several of the enhancements directly affect the GFMosiac algorithm. One of the most important changes to the TWINDS algorithm is the increase in horizontal resolution from 2 km to 1 km. This increase in resolution allows the algorithm to resolve the abrupt wind shifts associated with fronts and outflow boundaries much better (Figure 2). Previously, wind shifts associated with gust fronts would be excessively smoothed because of the coarse grid resolution coupled with the method the TWINDS algorithm uses to compute the wind speed and direction at each gridpoint.

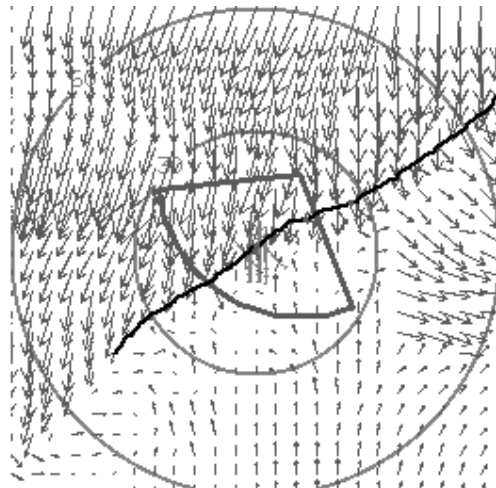


Figure 3. Terminal Winds data from September 21, 2000. Wind vectors are plotted at every third grid point and the solid line indicates the location of the cold front.

## 4. RESULTS

GFMosaic results from June 27, 2000 are shown in Figure 3. On this day, a strong convective outflow boundary approached DFW from the northwest. As the outflow boundary impacted the northern sections of the DFW AREAs Noted for Attention (ARENAs), portions of the front became radially aligned with both the DFW TDWR and DAL TDWR.

The DFW MIGFA (gust front algorithm using data from the DFW TDWR) was only able to detect the portion of the gust front from DFW airport to the west. This is where the velocity convergence associated with the front was still "visible" (Figure 3a). The location of the DAL TDWR inhibited the DAL MIGFA from detecting the velocity convergence in that location. Consequently, the detection from this algorithm only included the segment from the DFW airport to the north (Figure 3b). However, since the GF莫斯iac algorithm utilizes data from both radars it was able to capture the entire length of the gust front approaching DFW (Figure 3c).

Figure 4 shows the GF莫斯iac output from September 21, 2000. At this time, a strong cold front was crossing the DFW airport from northwest-to-southeast. The GF莫斯iac does as well as the DAL MIGFA (Figure 4b) and better than the DFW MIGFA (Figure 4a) in detecting the entire length of the front. Also, notice that the estimated post-frontal wind direction and speed provided by TWINDS (~360 deg, 15 m/s) agrees well with the values generated by MIGFA. The 15 m/s (~30 kts) estimate also corresponds well with the 25-30 kt wind gusts recorded by the LLWAS-NE centerfield wind sensor at DFW following the frontal passage.

A preliminary scoring exercise was performed to quantify the ability of the GF莫斯iac algorithm to identify and track gust fronts. The Probability of Detection (POD) and the Probability of False Alarm (PFA) were computed for three separate cases in order to gauge the algorithm's performance. The three cases represent three different types of weather conditions that can give rise to significant gust fronts.

The combined scores from the three cases (Table 1) show that the GF莫斯iac algorithm outperforms or equals the performance of the DFW MIGFA and DAL MIGFA in all of the strength categories. The GF莫斯iac algorithm has a better POD score in the detection of weaker gust fronts (0-10 m/s convergence category). This is important because these are the types of fronts that are especially difficult to detect when they become radially aligned.

The false detection probability (PFA) for GF莫斯iac is slightly higher than for either of the MIGFA algorithms. Additional parameter tuning and validity tests (e.g., requiring supporting evidence in terminal winds data) are being explored in order to help reject false interest features from the mosaic.

## **5. CONCLUSIONS**

The GFMosiac algorithm is a pre-planned product improvement (P3I) for the Integrated Terminal Weather System that will provide an improved gust front detection capability for TRACONs served by multiple Doppler radars. The algorithm has recently been enhanced to ingest wind fields from the Terminal Winds algorithm. The TWINDS data provide useful wind shear and pre- and post-frontal wind information that are used by the GF莫斯 algorithm to validate or reject candidate gust front detections, as well as contributing to the final wind shift and wind shear reports that are reported to air traffic controllers.

Preliminary scoring results showed that the GFMosiac algorithm improved the POD of gust fronts at DFW for three separate cases. However, an increase in the POD also led to an increase in the PFA for the same events. Work is continuing to fine-tune the parameter set to maintain the improved detection performance while reducing the number of false alarms.

## **6. REFERENCES**

- Delanoy, R.L., J.G. Verly, and D.E. Dudgeon, 1992: "Functional templates and their application to 3-D object recognition," Proceedings of the 1992 International Conference of Acoustics, Speech, and Signal Processing, San Francisco, CA, March 23-26, 1992.
- Delanoy, R.L., and S.W. Troxel, 1993: "Machine intelligent gust front detection", Lincoln Laboratory Journal, Vol. 6, No. 1, 187-211, 1993.
- Evans, J.E., E.R. Ducot 1994: The Integrated Terminal Weather System (ITWS). Lincoln Laboratory Journal, Vol. 7, No. 2.
- Troxel, S.W. and R.L. Delanoy, 1994: "Machine intelligent approach to automated gust front detection for Doppler weather radars", SPIE Proceedings: Sensing, Imaging, and Vision for Control and Guidance of Aerospace Vehicles, Volum 2220, 182-193, April, 1994
- Troxel, S.W., R.L. Delanoy, J.P. Morgan, W.L. Pughe: Machine intelligent gust front algorithm for the Terminal Doppler Weather Radar (TDWR) and Integrated Terminal Weather System (ITWS), AMS Workshop on Wind Shear and Wind Shear Alert Systems, 70-79, November, 1996, Oklahoma City, OK.

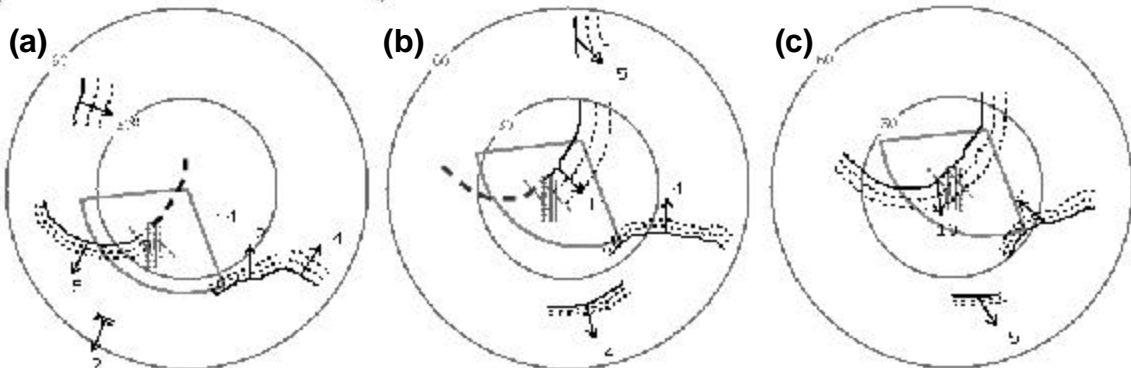


Figure 4. Gust front detections from the DFW MIGFA (a), DAL MIGFA (b), and the GFMosiac algorithm (c) for June 27, 2000 at 1957 UTC. The solid and thin dashed lines indicate gust front locations and future positions respectively. The thick dashed line illustrates the portion of the gust front that is not detected due to radial alignment. The thick dashed lines in (a) and (b) illustrate the portion of the gust front that is not being detected due to radial alignment. The runways indicate the location of the TDWR airport and the pie-shaped wedge represents the DFW hazardous sector scan covered by the DFW TDWR.

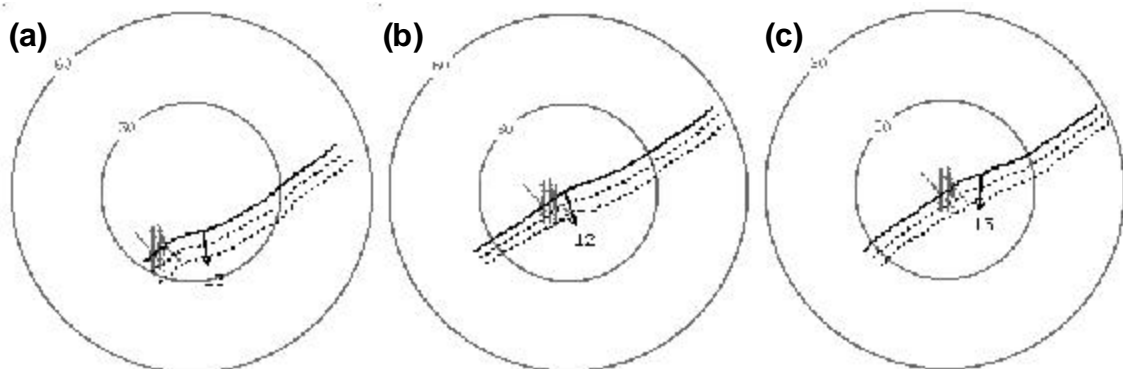


Figure 5. Gust front detections from the DFW MIGFA (a), DAL MIGFA (b), and the GFMosiac algorithm, for September 21, 2000 at 0100 UTC. The solid and dashed lines indicate gust front locations and future positions, respectively. The arrow and number represent the wind direction and speed that can be expected 10 minutes after the frontal passage.

Table 1. Performance Comparisons of Individual MIGFAs and GFMosiac at DFW. Probability of Detection (POD) statistics are broken down by convergence strength.

	POD					PFA
	0 - 10 m/s	10 - 15 m/s	15 - 25 m/s	>= 25 m/s	ALL	
DFW MIGFA	0.78 (85/109)	0.97 (29/30)	0.0 (0/0)	1.0 (24/24)	.85 (138/163)	.21 (58/281)
DAL MIGFA	0.88 (95/108)	1.0 (31/31)	0.0 (0/0)	1.0 (22/22)	.92 (148/161)	.22 (75/340)
GFMosiac	0.97 (89/92)	1.0 (30/30)	0.0 (0/0)	1.0 (23/23)	.98 (142/145)	.26 (119/460)